Acta Cryst. (1997). B53, 25–31

Pressure-Induced $Fm\bar{3}m \rightarrow R\bar{3}$ Phase Transition in $NaSbF_6$

H. Sowa

Institut für Mineralogie, Petrologie und Kristallographie der Philipps-Universität Marburg, Hans-Meerwein-Strasse, D-35032 Marburg, Germany

(*Received 20 May 1996; accepted 27 August 1996*)

Abstract

High-pressure X-ray diffraction measurements on $NaSbF_6$ powder were performed up to 5.63 (7) GPa. At ~ 0.1 GPa the cubic low-pressure phase with ordered ReO_3-type crystal structure undergoes a phase transition into a rhombohedral $LiSbF_6$-type modification. The high-pressure behaviour of this phase is characterized by rotations and distortions of the coordination octahedra, but it also can be described with a sphere-packing deformation. The octahedral distortions are probably caused by cation–cation repulsions.

1. Introduction

$NaSbF_6$ crystallizes in the cubic space group $Fm\bar{3}m$ with lattice parameter $a = 8.184\,(5)$ Å (Teufer, 1956). The structure is built up by corner-linked NaF_6 and SbF_6 octahedra. It can be described as an ordered ReO_3-type structure.

The high-temperature phases for many fluorides with di- and tetravalent cations show the $NaSbF_6$ structure type. These compounds often undergo phase transitions into modifications with the rhombohedral ($R\bar{3}$) low-temperature $LiSbF_6$ structure type. Such phase transitions were the subject of the work of Reinen & Steffens (1978). Especially $CoZrF_6$ and $ZnZrF_6$ were extensively investigated by Rodriguez, Couzi, Tressaud, Grannec, Chaminade & Soubeyroux (1990), Rodriguez, Couzi, Tressaud, Grannec, Chaminade & Ecolivet (1990), Rodriguez, Couzi, Sourisseau, Tressaud, Grannec, Chaminade, Soubeyroux & Ecolivet (1991) and Gorev, Flerov, Tressaud, Grannec, Rodriguez & Couzi (1992). The $Fm\bar{3}m \rightarrow R\bar{3}$ phase transition is described by means of Landau theory (Rodriguez & Couzi, 1990). It is considered as 'improper' ferroelastic, driven by octahedral rotations. Internal strains induced by the rotations cause the rhombohedral distortion of the unit cell and small deformations of the coordination octahedra. None of these compounds have been examined structurally under high pressure.

2. Experimental

Sodium hexafluoroantimonate was obtained from Aldrich Chemie, Germany. Dissolving the sample in ethanol made it possible to remove insoluble impurities. Cube-shaped single crystals of $NaSbF_6$ up to 0.1 mm^3 in size could be obtained by recrystallization from the solution.

Table 1. *Structural parameters of $NaSbF_6$ at ambient conditions*

	x	y	z	U^{11} (Å^2)	U^{22} (Å^2) = U^{33} (Å^2)
Sb	0	0	0	0.0225 (4)	
Na	1/2	1/2	1/2	0.029 (2)	
F	0.2260 (8)	0	0	0.025 (3)	0.127 (5)

Teufer (1956) reported only isotropic displacement factors. Therefore, it was useful to redetermine the crystal structure. For this purpose a crystal of approximately 90 × 90 × 50 µm^3 was selected. Since $NaSbF_6$ is hygroscopic the single-crystal study at ambient pressure was performed with the crystal covered with a small amount of vaseline inside a Merrill–Bassett-type diamond–anvil cell (Merrill & Bassett, 1974). The crystal-structure variations under high pressure could not be measured using a single-crystal technique because a phase transition destroying the crystal occurred at very low pressure.

All high-pressure investigations were performed on powder samples using a lever-arm diamond–anvil cell (opening angle 30°). The pressure-transmitting medium was Fluorinert and the experiments were carried out with Mo $K\alpha_1$ ($\lambda = 0.7093$ Å, quartz monochromator) and Mo $K\beta$ ($\lambda = 0.6392$ Å, Si monochromator) radiation in a Debye–Scherrer film technique (camera radius 45 mm). The pressure was calibrated with the ruby-fluorescence method (Piermarini, Block, Barnett & Forman, 1975).

3. Results

The results of the single-crystal data refinements (47 independent reflections) are given in Table 1.*

As has been observed in isotypic compounds (*e.g.* Rodriguez, Couzi, Tressaud, Grannec, Chaminade & Soubeyroux, 1990) the F atoms show strong anisotropic

---

* A list of structure factors has been deposited with the IUCr (Reference: SE0203). Copies may be obtained through The Managing Editor, International Union of Crystallography, 5 Abbey Square, Chester CH1 2HU, England.

© 1997 International Union of Crystallography
Printed in Great Britain – all rights reserved

Table 2. *Lattice parameters of $NaSbF_6$ at various pressures*

	Rhombohedral F, pseudo-cubic		Rhombohedral P		Hexagonal			
P (GPa)	a_p (Å)	α_p (°)	a_r (Å)	α_r (°)	a_h (Å)	c_h (Å)	c/a	V (Å^3)
0.0001*	8.203 (1)	90	5.800	60	5.800	14.208	2.4495	414.0 (2)
0.09*	~8.15	90	5.76	60	5.76	14.12	2.4495	406
0.09†	8.024 (2)	87.57 (3)	5.793 (7)	57.27 (6)	5.552 (2)	14.475 (5)	2.6072	386.5 (4)
0.11	7.993 (2)	86.80 (2)	5.808 (5)	56.44 (5)	5.492 (1)	14.597 (5)	2.6579	381.3 (3)
0.26	7.914 (3)	85.62 (4)	5.81 (1)	55.19 (9)	5.378 (3)	14.716 (9)	2.7363	368.6 (6)
0.57	7.834 (2)	84.81 (2)	5.785 (5)	54.34 (5)	5.283 (1)	14.747 (5)	2.7914	356.4 (3)
0.72	7.791 (4)	84.57 (5)	5.76 (1)	54.1 (1)	5.242 (3)	14.715 (13)	2.8071	350.2 (7)
0.94	7.771 (6)	84.08 (7)	5.762 (9)	53.73 (7)	5.208 (2)	14.748 (7)	2.8318	346.4 (5)
1.32	7.719 (3)	83.80 (3)	5.746 (9)	53.31 (8)	5.155 (2)	14.744 (7)	2.8601	339.3 (4)
1.72	7.685 (5)	83.66 (6)	5.73 (2)	53.2 (1)	5.125 (4)	14.708 (14)	2.8699	334.6 (8)
1.85	7.667 (4)	83.58 (4)	5.72 (1)	53.1 (1)	5.109 (3)	14.690 (9)	2.8753	332.1 (5)
3.04	7.577 (3)	83.29 (3)	5.662 (8)	52.80 (7)	5.035 (2)	14.578 (8)	2.8953	320.1 (4)
3.17	7.583 (7)	83.22 (8)	5.67 (2)	52.7 (2)	5.035 (5)	14.60 (2)	2.9001	321 (1)
3.62	7.562 (6)	83.21 (8)	5.66 (2)	52.7 (2)	5.021 (4)	14.57 (2)	2.9001	318.0 (9)
3.77	7.551 (2)	83.16 (2)	5.648 (7)	52.67 (6)	5.011 (2)	14.552 (7)	2.9040	316.5 (4)
5.63	7.443 (7)	83.0 (1)	5.57 (2)	52.6 (2)	4.934 (4)	14.37 (3)	2.9118	303 (1)
0.51‡	7.851 (3)	84.89 (4)	5.793 (9)	54.43 (8)	5.299 (2)	14.759 (7)	2.7852	358.9 (5)
0.17	7.980 (2)	86.48 (3)	5.813 (7)	56.09 (7)	5.467 (2)	14.646 (6)	2.6790	379.1 (4)
0.05	8.048 (4)	87.37 (6)	5.82 (2)	57.1 (1)	5.559 (4)	14.564 (9)	2.6199	389.7 (9)
>0.0001	8.102 (6)	88.12 (7)	5.82 (2)	57.9 (2)	5.634 (7)	14.485 (11)	2.5710	398 (1)

* Cubic phase. † Increasing pressure. ‡ Decreasing pressure.

thermal displacement factors, indicating a dynamic disorder and non-linear Na—F—Sb bonds. The nonlinearity of these bonds gives rise to a cubic lattice parameter a that is considerably shorter than the sum of ionic radii (Shannon, 1976).

Table 2 gives the results of the high-pressure measurements on $NaSbF_6$ powder.

The phase transition from the cubic low-pressure phase ($Fm\bar{3}m$) into the rhombohedral high-pressure phase ($R\bar{3}$) already took place at very low pressure. A Debye–Scherrer photograph taken at 0.09 GPa showed powder lines of both phases. The a lattice parameter of the cubic modification could only be estimated roughly. The volume of the unit cell is reduced by $\sim 2\%$ compared with the uncompressed compound.

The structure of the high-pressure phase can be described in different ways: usually the rhombohedral primitive cell is reported on. Table 2 also gives the corresponding hexagonal unit cell with triple volume. In addition, the rhombohedral face-centered cell with quadruple volume is shown in order to compare the cubic low-pressure phase with the high-pressure phase. It is possible to describe the cubic structure with each of these settings. The formulae for the unit-cell transformations are given by Rodriguez, Couzi, Tressaud, Grannec, Chaminade & Soubeyroux (1990).

Considering the lattice parameters of the rhombohedral P cell it can be stated that a_r shortens continuously with increasing pressure. At the transition pressure the rhombohedral angle is $\alpha_r \simeq 57.3°$. Under high pressure it is reduced and seems to approach a final value of 52.6°. With regard to the hexagonal unit cell an uncommon behaviour becomes obvious. Whereas the a_h parameter decreases continuously with increasing pressure (Fig. 1), the c_h parameter increases up to ~ 0.7 GPa, passes a maximum and decreases subsequently (Fig. 2). The axial ratio increases under high pressure and approaches a final value of $c/a \simeq 2.91$. Fig. 3 shows the volume of the hexagonal unit cell *versus* pressure.

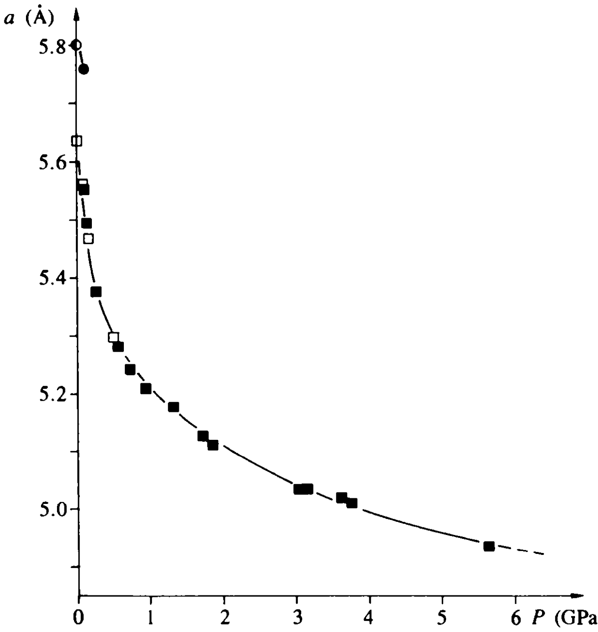

Fig. 1. Hexagonal a lattice parameter of $NaSbF_6$ *versus* pressure ○● cubic phase, ■□ rhombohedral phase, ■● increasing pressure, □○ decreasing pressure.

The phase transition shows a hysteresis: With increasing pressure the transformation took place at approximately 0.1 GPa, whereas on decompression the rhombohedral high-pressure phase could be retained to almost ambient conditions. However, after the pressure cell was opened only cubic $NaSbF_6$ existed.

4. Discussion

For an easier understanding of the high-pressure behaviour of $NaSbF_6$ it is useful to regard first the ReO_3 structure type. Megaw (1968) recognized that it is theoretically possible to distort the perovskite-type structure of $LiNbO_3$ by cooperative rotations of the NbO_6 octahedra around one of their triad axes into a structure with hexagonally close-packed O atoms. Many further papers also deal with such octahedral tiltings in perovskite-type structures. Geometrical details are given by, *e.g.*, Moreau, Michel, Gerson & James (1970) and Megaw & Darlington (1975).

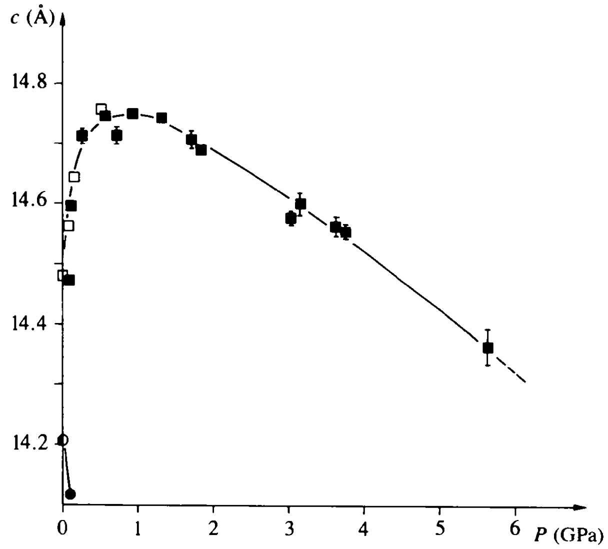

Fig. 2. Hexagonal *c* lattice parameter of $NaSbF_6$ *versus* pressure. For symbols see Fig. 1.

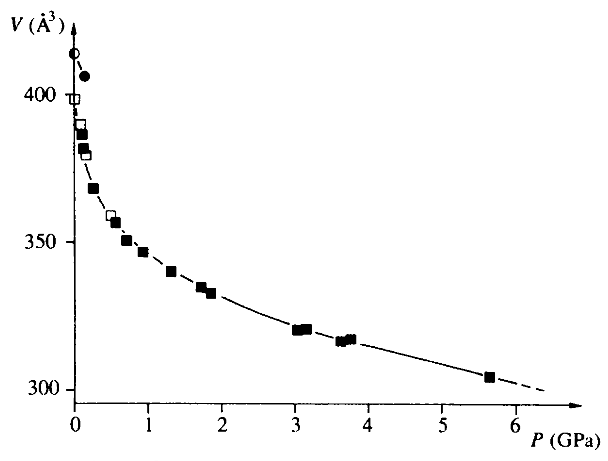

Fig. 3. Volume of the hexagonal unit cell of $NaSbF_6$ *versus* pressure. For symbols see Fig. 1.

4.1. *AX₃ compounds*

The octahedral arrangement in ReO_3-type structures ($Pm\bar{3}m$) is the same as in ideal perovskite and therefore the tilts of the octahedra may also result in a hexagonal close anion packing, as has been investigated for trifluorides AF_3 by Michel, Moreau & James (1971). The octahedral rotations give rise to a phase transition from the ReO_3 structure type into the VF_3 structure type with the symmetry $R\bar{3}c$. Compounds with different chemical composition show different rotation angles. The structure type with the maximum rotation angle has a hexagonally close-packed anion arrangement and is termed the PdF_3 type.

Such structural changes may also be interpreted as a sphere-packing deformation: The arrangement of the O atoms in ReO_3 [Wyckoff position (3*d*) $\frac{1}{2}$,0,0 in $Pm\bar{3}m$] corresponds to a configuration of the cubic invariant lattice complex *J* (*International Tables for Crystallography*, 1992, Vol. A) and to a sphere packing of the type 8/3/*c*2, with eight contacts per sphere (Fischer, 1973). For the symmetry reduction from $Pm\bar{3}m$ to $R\bar{3}c$ two intermediate subgroups are possible (*cf.* Fig. 4): (1) $Fm\bar{3}c$ is a class-equivalent subgroup with doubled lattice parameter *a*. The *J* configuration occurs in the invariant position (24*c*) $\frac{1}{4}$,0,0. $R\bar{3}c$ is a translational-equivalent subgroup of $Fm\bar{3}c$. In the follwing $R\bar{3}c$ is described with a hexagonal unit cell. (2) $R\bar{3}m$ is a translational-equivalent subgroup of $Pm\bar{3}m$. The *J* configuration is found in position (9*d*) $\frac{1}{2}$,0,$\frac{1}{2}$ (hexagonal unit cell). The unit cell shows cubic metrics with $c/a = 6^{1/2}/2 \simeq 1.2247$. $R\bar{3}c$ is a class-equivalent subgroup of $R\bar{3}m$ with doubled lattice parameter *c*. In $R\bar{3}c$ the ideal *J* configuration occurs in position (18*e*) $x,0,\frac{1}{4}$ with $x = \frac{1}{2}$ and $c/a = 6^{1/2}$.

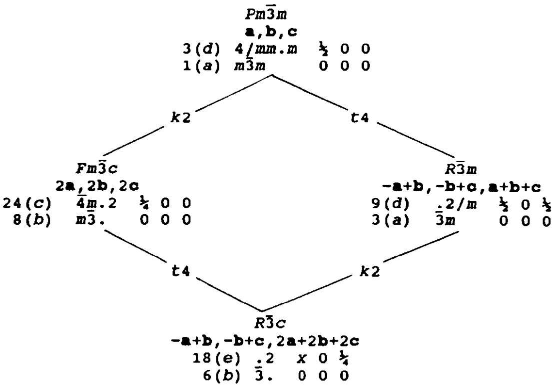

Fig. 4. Symmetry relations between ReO_3 and VF_3 structure types. Positions that are occupied by anions and cations are given [O in ReO_3 in (3*d*), Re in (1*a*)].

In $R\bar{3}c$ the sphere packing 8/3/c2 may be deformed without losing contacts if the following condition is fulfilled (Fischer, 1992)

$$x = \frac{1}{2} \pm [(c^2/72a^2) - 1/12]^{1/2}.$$

At positional parameters $x,0,\frac{1}{4}$ with $x = \frac{1}{3}$ and an axial ratio $c/a = 8^{1/2} \simeq 2.828$, the arrangement of a hexagonal close packing with 12 contacts per sphere is reached as a limiting form. Fig. 5 shows some compounds with anion arrangements corresponding to a deformed sphere packing 8/3/c2 [data from *Structure Reports* (1980–1992), edited by G. Ferguson, Vols. 44A–57A]. During the deformation the density of the ideal sphere packing increases from $\rho = 55.5\%$ in the *J* configuration to $\rho = 74.1\%$ in the hexagonal close packing and the ideal octahedral voids around (6*b*) 000 are maintained, while cuboctahedral voids split up into octahedral and tetrahedral interstices.

It may be expected that the ReO_3-type structure should be stable at high temperatures, whereas the PdF_3 structure type should occur as a high-pressure phase. In fact, phase transitions from the rhombohedral low-temperature phase into the cubic high-temperature phase have been observed in many AF_3 (*A* = Al, Cr, Ga, V, Fe, In, Ti) compounds (Ravez, Mogus-Milankovic, Chaminade & Hagenmuller, 1984; Mogus-Milankovic, Ravez, Chaminade & Hagenmuller, 1985; Daniel, Bulou, Leblanc, Rousseau & Nouet, 1990; Daniel, Bulou, Rousseau, Fourquet, Nouet & Leblanc, 1990; Daniel, Bulou, Rousseau, Nouet & Leblanc, 1990).

A neutron diffraction study up to 7.2 GPa on AlD_3 (VF_3-type) reveals that the D atoms build up a hexagonal close packing at high pressure (Goncharenko Glazkov, Irodova & Somenkov, 1991).

4.2. *ABX_6 compounds*

The $NaSbF_6$ structure type ($Fm\bar{3}m$) also can be derived from the ReO_3 type (Fig. 6): $Fm\bar{3}m$ is a class-equivalent subgroup of $Pm\bar{3}m$ with doubled lattice parameter *a*. The ideal *J* configuration occurs in position (24*e*) $x,0,0$ with $x = \frac{1}{4}$. Small deviations of the ideal *x* parameter result in two types of octahedra with different sizes around (4*a*) 000 and (4*b*) $\frac{1}{2}\frac{1}{2}\frac{1}{2}$, respectively. Further symmetry reduction leads to the translational-equivalent subgroup $R\bar{3}m$ of $Fm\bar{3}m$. Here the ideal *J* configuration occurs in position (18*h*) $x,\bar{x},z$ ($x = 0.16666$, $z = 0.08333$, $c/a = 6^{1/2}$, hexagonal unit cell). The symmetry $R\bar{3}m$ does not allow rotations, only distortions of the octahedra around (3*a*) 000 and (3*b*) $00\frac{1}{2}$. Octahedral tilting is possible in the translational-equivalent subgroup $R\bar{3}$ of $R\bar{3}m$. The anions in the corresponding $LiSbF_6$ structure type occupy the general

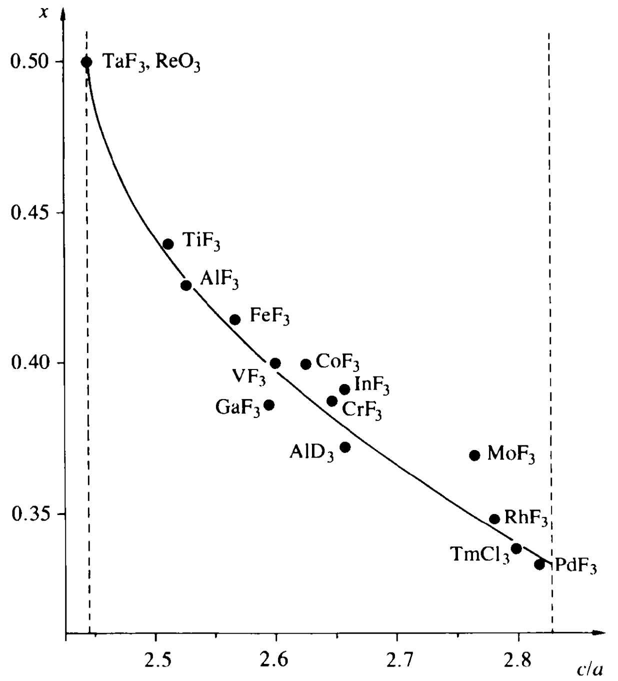

Fig. 5. Rhombohedral deformation of a sphere packing of the type 8/3/c2 in $R\bar{3}c$. The solid line represents the parameters fulfilling the sphere-packing condition. Compounds with anion arrangements almost corresponding to the sphere packing are given.

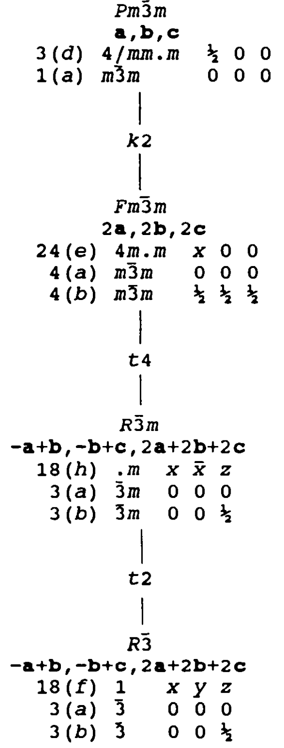

Fig. 6. Symmetry relations between ReO_3, $NaSbF_6$ and $LiSbF_6$ structure types. Positions that are occupied by anions and cations are given.

position (18*f*) x,y,z (hexagonal unit cell). The ideal J configuration is obtained at $x=\frac{1}{2}$, $y=0$, $z=\frac{1}{4}$ and $c/a=6^{1/2}$. As shown in Fig. 7, the LiSbF$_6$ type can be derived from the VF$_3$ type. While in the VF$_3$ structure type all octahedra are symmetrically equivalent, LiSbF$_6$-type structures show two different types of octahedra and the fluorine arrangement deviates slightly from the ideal sphere packing.

At the pressure-induced phase transition in NaSbF$_6$ a sudden increase of c_h was observed (Fig. 2) that corresponds to the elongation of the c_h parameter at the temperature-dependent phase transition in isotypic compounds with di- and tetravalent cations (Reinen & Steffens, 1978; Rodriguez, Couzi, Tressaud, Grannec, Chaminade & Soubeyroux, 1990). This behaviour can be explained as an effect of the disorder of the cubic structure that shows non-linear cation–anion–cation bonds. Information on the geometrical details of the LiSbF$_6$-type crystal structure can be derived indirectly from the lattice parameters if the cation–anion bond lengths are known. Using the formulae given by Reinen & Steffens (1978) it can be shown that at the transition pressure the rhombohedral NaSbF$_6$ modification contains almost ideal NaF$_6$ and SbF$_6$ octahedra with Na—F and Sb—F bond lengths corresponding to the ionic radii (Shannon, 1976). At this pressure the hexagonal c_h parameter corresponds to the body diagonal of a cubic unit cell with linear Na—F—Sb bonds. For the following considerations it was assumed that the cation–anion bond distances did not change under pressure.

The compression mechanism in rhombohedral NaSbF$_6$ is the same as may occur in VF$_3$-type structures. Just as in the VF$_3$ structure type, the octahedral rotations in NaSbF$_6$ should leave the hexagonal c_h parameter constant, while a_h should be shortened. Therefore, the observed elongation of c_h under pressure must originate from octahedral distortions. Each octahedron shows two symmetrically non-equivalent F—F distances (Fig. 8). While the octahedra rotate around [001] the difference in the lengths of d_1 and d_2 and d'_1 and d'_2, respectively, increases up to ~ 0.6 GPa. It is probable that the NaF$_6$ octahedra are more distorted than the SbF$_6$ octahedra due to the highly charged Sb^{5+} cations. In the range between 0.6 and 1.5 GPa there are only rotations, but no further distortions of the octahedra. Above 1.5 GPa the differences in the F—F distances become reduced.

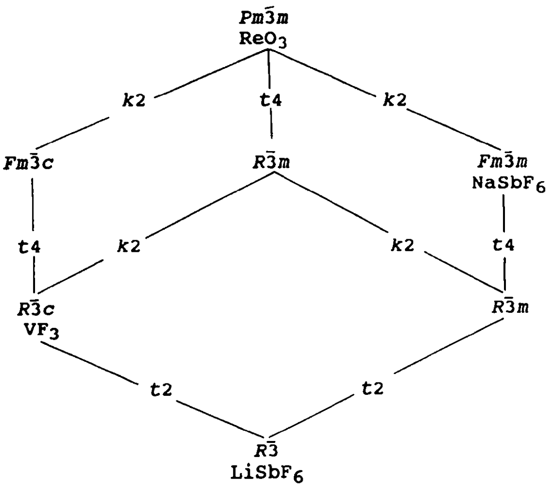

Fig. 7. Symmetry relations between ReO$_3$-, VF$_3$-, NaSbF$_6$- and LiSbF$_6$ structure types.

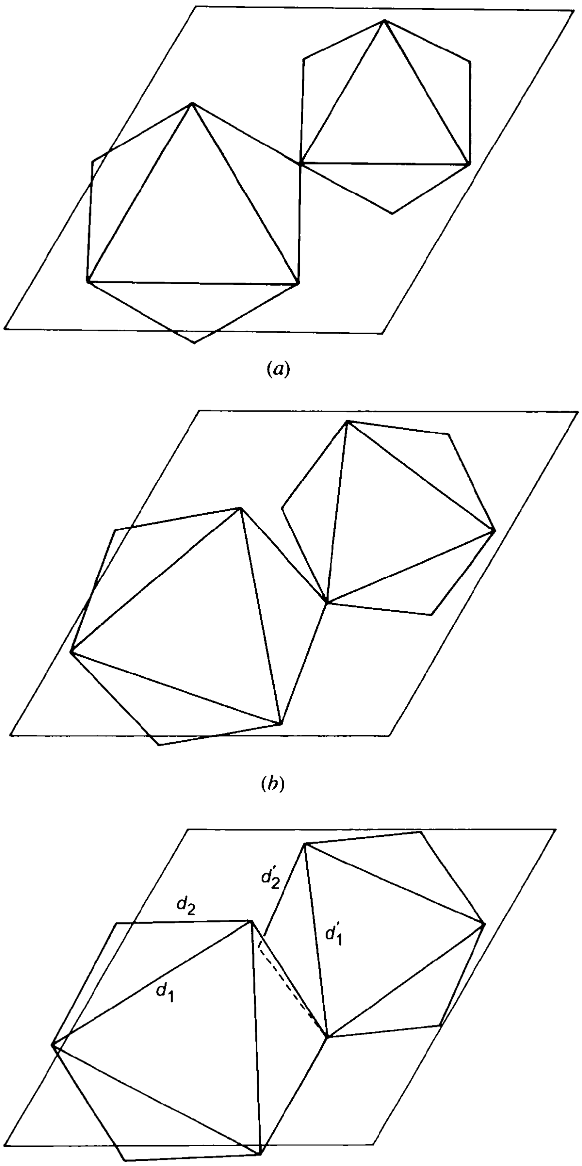

(*a*)

(*b*)

(*c*)

Fig. 8. Octahedral rotations in NaSbF$_6$ under high pressure: (*a*) cubic phase, projection ∥ [111], hexagonal axes are given; (*b*), (*c*) rhombohedral phase, projection ∥ [001] (hexagonal unit cell). d_1, d_2 and d'_1, d'_2 indicate the two different F—F distances per octahedron.

A similar effect has also been observed in $CoZrF_6$ and $ZnZrF_6$ at low temperatures (Rodriguez, Couzi, Tressaud, Grannec, Chaminade & Soubeyroux, 1990; Rodriguez, Couzi, Tressaud, Grannec, Chaminade & Ecolivet, 1990). However, the pressure-induced effect is much stronger than the temperature-dependent changes and the octahedral distortions must not be neglected.

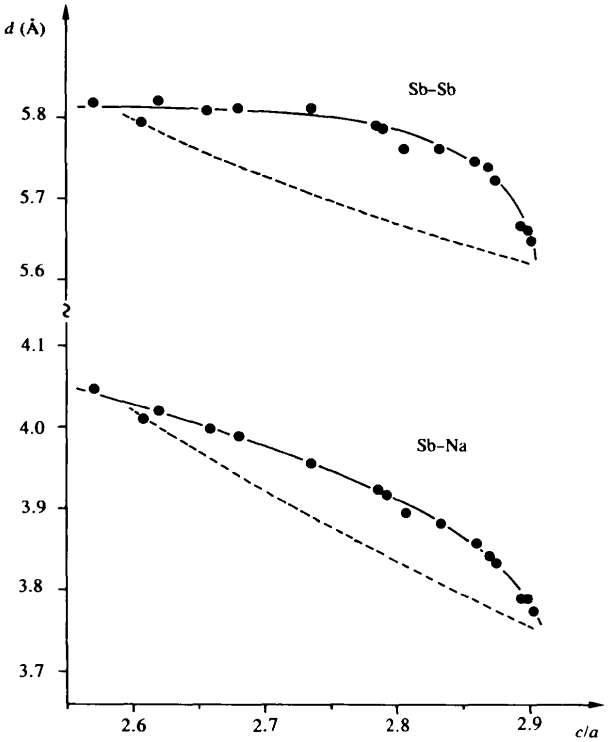

Fig. 9. Experimentally determined distances between cations in $NaSbF_6$ *versus* the axial ratio c/a. The corresponding distances referring to a theoretical structure model with regular octahedra are represented by dashed lines.

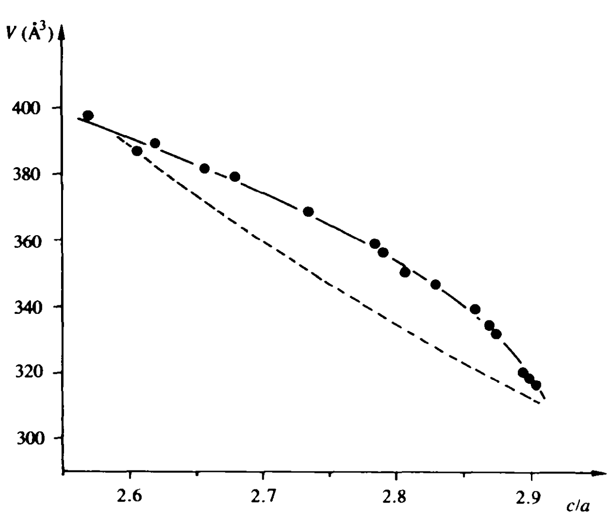

Fig. 10. Volume of the hexagonal unit cell of $NaSbF_6$ *versus* the axial ratio. The dashed line shows the volume changes according to a theoretical structure model with regular octahedra.

Probably these distortions are caused by repulsions between the cations, particularly between the Sb cations. Fig. 9 shows experimentally determined cation–cation distances *versus* the axial ratio of the hexagonal unit cell. The dashed lines represent the corresponding distances in a theoretical structure model with tilted regular octahedra. The real crystal structure shows clearly longer Sb—Sb and Na—Sb distances than the theoretical model with undistorted octahedra. Only when the final c/a ratio is reached would there no longer be a difference. In order to avoid too short distances between the cations the crystal structure suffers octahedral distortions. The cation–cation distances which have been observed under pressure would lead in the theoretical crystal structure with regular octahedra to much smaller c/a ratios and a less dense anion packing. For example: at a pressure of 0.9 GPa the observed Sb—Sb distance along the rhombohedral a direction is $d \simeq 5.75$ Å, the hexagonal unit cell has an axial ratio of $c/a \simeq 2.83$ and its volume is $V \simeq 345$ Å^3. The structure model with undistorted octahedra shows identical Sb—Sb distances at $c/a \simeq 2.64$. The corresponding unit-cell volume is $V \simeq 375$ Å^3 (Figs. 9 and 10), which is ~ 8.5% larger than observed.

Summing up, it may be said that the high-pressure behaviour of the rhombohedral modification of $NaSbF_6$ can be described as a deformation of a slightly distorted sphere packing of type 8/3/c2 of the anions, which is superimposed by the cation–cation repulsions.

I thank Professors E. Koch and W. Fischer for helpful discussions. This work was supported by the Deutsche Forschungsgemeinschaft under So 276/1.

References

Daniel, P., Bulou, A., Leblanc, M., Rousseau, M. & Nouet, J. (1990). *Mater. Res. Bull.* **25**, 413–420.

Daniel, Ph., Bulou, A., Rousseau, M., Fourquet, J. L., Nouet, J. & Leblanc, M. (1990). *J. Phys. Condens. Matter*, **2**, 5663-5677.

Daniel, P., Bulou, A., Rousseau, M., Nouet, J. & Leblanc, M. (1990). *Phys. Rev. B*, **42**, 10545-10552.

Fischer, W. (1973). *Z. Kristallogr.* **138**, 129–146.

Fischer, W. (1992). Personal communication.

Goncharenko, I. N., Glazkov, V. P., Irodova, A. V. & Somenkov, V. A. (1991). *Phys. B*, **174**, 117-120.

Gorev, M. V., Flerov, I. N., Tressaud, A., Grannec, J., Rodriguez, V. & Couzi, M. (1992). *Phys. Status Solidi B*, **169**, 65-71.

Megaw, H. D. (1968). *Acta Cryst.* **A24**, 583-588.

Megaw, H. D. & Darlington, C. N. W. (1975). *Acta Cryst.* **A31**, 161-173.

Merrill, L. & Bassett, W. A. (1974). *Rev. Sci. Instrum.* **45**, 290–294.

Michel, C., Moreau, J. M. & James, W. J. (1971). *Acta Cryst.* **B27**, 501-503.

Mogus-Milankovic, A., Ravez, J., Chaminade, J. P. & Hagenmuller, P. (1985). *Mater. Res. Bull.* **20**, 9–17.

Moreau, J.-M., Michel, C., Gerson, R. & James, W. J. (1970). *Acta Cryst.* B**26**, 1425–1428.

Piermarini, G. J., Block, S., Barnett, J. D. & Forman, R. A. (1975). *J. Appl. Phys.* **46**, 2774–2780.

Ravez, J., Mogus-Milankovic, A., Chaminade, J. P. & Hagenmuller, P. (1984). *Mater. Res. Bull.* **19**, 1311–1316.

Reinen, D. & Steffens, F. (1978). *Z. Anorg. Allg. Chem.* **441**, 63–82.

Rodriguez, V. & Couzi, M. (1990). *J. Phys. Condens. Matter*, **2**, 7395–7406.

Rodriguez, V., Couzi, M., Sourisseau, C., Tressaud, A., Grannec, J., Chaminade, J. P., Soubeyroux, J. L. & Ecolivet, C. (1991). *Phase Transit.* **33**, 85–90.

Rodriguez, V., Couzi, M., Tressaud, A., Grannec, J., Chaminade, J. P. & Ecolivet, C. (1990). *J. Phys. Condens. Matter*, **2**, 7387–7394.

Rodriguez, V., Couzi, M., Tressaud, A., Grannec, J., Chaminade, J. P. & Soubeyroux, J. L. (1990). *J. Phys. Condens. Matter*, **2**, 7373–7386.

Shannon, R. D. (1976). *Acta Cryst.* A**32**, 751–767.

Teufer, G. (1956). *Acta Cryst.* **9**, 539–540.